Ocean Modelling 183 (2023) 102197

Contents lists available at ScienceDirect

Ocean Modelling

journal homepage: www.elsevier.com/locate/ocemod

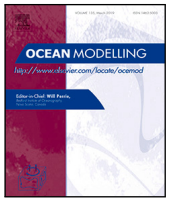

Sandy beach dynamics by constrained wave energy minimization

Ronan Dupont [a,b,c,*], Megan Cook [a,b,c], Frédéric Bouchette [a,c], Bijan Mohammadi [b,c], Samuel Meulé [a,c]

[a] GEOSCIENCES-M, Univ Montpellier, CNRS, Montpellier, France
[b] IMAG, Univ Montpellier, CNRS, Montpellier, France
[c] GLADYS, Univ Montpellier, Le Grau-du-Roi, France

ARTICLE INFO

Keywords:
Hydro-morphodynamics
Optimization
Model validation
Coastal
Variational approach
Energy minimization
Optimal transport
Waves

ABSTRACT

This paper focuses on a new approach to describe coastal morphodynamics, based on optimization theory, and more specifically on the assumption that a sandy beach profile evolves in order to minimize a wave-related function, the choice of which depends on what is considered the driving force behind the coastal morphodynamic processes considered. The numerical model derived from this theory uses a gradient descent method and allows us to account for physical constraints such as sand conservation in wave flume experiments. Hence, the model automatically adapts to either wave flume or open sea settings and only involves two hyper-parameters: a sand mobility and a critical angle of repose. The ability of OptiMorph to model cross-shore beach morphodynamics is illustrated on a flume configuration. Comparison of the beach profile changes computed with OptiMorph with experimental data as well as the results from the coastal morphodynamic software XBeach demonstrates the potential of a model by wave energy minimization.

1. Introduction

Optimization theory is the study of the evolution of a system while searching systematically for the minimum of a function derived from physical properties of the system. In this paper, we have applied this approach to coastal dynamics, with our primary objective to simulate the interactions between the waves and the sea bottom along a cross-shore profile. Using mathematical optimization theory (Isèbe et al., 2014; Isebe et al., 2008; Isèbe et al., 2008; Bouharguane et al., 2010; Bouharguane and Mohammadi, 2012; Mohammadi and Bouharguane, 2011; Mohammadi and Bouchette, 2014; Mohammadi, 2017; Cook et al., 2021), we have designed a model that describes the evolution of the sea bottom while taking into account the coupling between morphodynamic and hydrodynamic processes. This study focuses on a theoretical and numerical approach to the modeling of this coupling, based on the assumption that the beach profile adapts to minimize a certain wave-related function. The choice of this function determines the driving force behind the morphological evolution of the beach profile. This optimization problem is subjected to a certain number of constraints, allowing for a more accurate description of the morpho-dynamic evolution. This study is accompanied by the development of a numerical hydro-morphodynamic model, which has the advantages of being fast, robust, and of low complexity. The model was given the name *OptiMorph*.

The paper starts with a description of the simple hydrodynamic model used to calculate the driving forces behind the morphodynamic processes. Then, we provide a description of the morphodynamic model OptiMorph based on wave-energy minimization. With the purpose of validating OptiMorph, we compare the results of the numerical simulation with that of experimental data acquired in a flume experiment. We also compare the model to another nearshore hydro-morphodynamic model, XBeach (Roelvink et al., 2009), to see how it fares against existing hydro-morphodynamic models, XBeach being considered to be quite a reputable model in the coastal dynamic community (Zimmermann et al., 2012; Bugajny et al., 2013; Williams et al., 2015).

1.1. State of the art

Numerical models of morphodynamic processes are seen as a valuable tool for understanding and predicting the evolution of the sediment transport of the morphology over time in coastal areas. Different morphodynamic models exist in the literature, ranging from empirical models (de Vriend et al., 1994; Gravens, 1997; Kana et al., 1999; Ruessink and Terwindt, 2000) to process-based models. The latter can be sorted into several categories, such as (i) profile evolution models

* Corresponding author at: GEOSCIENCES-M, Univ Montpellier, CNRS, Montpellier, France.
E-mail addresses: ronan.dupont@umontpellier.fr (R. Dupont), megan.cook@umontpellier.fr (M. Cook), frederic.bouchette@umontpellier.fr (F. Bouchette), bijan.mohammadi@umontpellier.fr (B. Mohammadi), meule@cerege.fr (S. Meulé).

https://doi.org/10.1016/j.ocemod.2023.102197
Received 3 March 2023; Received in revised form 6 April 2023; Accepted 8 April 2023
Available online 16 April 2023
1463-5003/© 2023 The Author(s). Published by Elsevier Ltd. This is an open access article under the CC BY-NC-ND license (http://creativecommons.org/licenses/by-nc-nd/4.0/).

(Larson and Kraus, 1989; Larson et al., 1990; Nairn and Southgate, 1993), which use only cross-shore transport, (ii) rules-based models (Storms et al., 2002; McCarroll et al., 2021), based on a number of rules such as Brunn's rule (Bruun, 1954), (iii) 2D morphological models (Fleming and Hunt, 1977; Latteux, 1980; Coeffe and Pechon, 1982; Yamaguchi and Nishioka, 1985; Watanabe et al., 1986; Maruyama and Takagi, 1988; Wang et al., 1993; Johnson et al., 1995; Nicholson et al., 1997; Roelvink et al., 2009), which use depth-averaged wave and current equations to model the sediment transport while neglecting the vertical variations of wave-derived parameters, as well as (iv) 3D and quasi-3D models (Roelvink et al., 1994; Lesser et al., 2004; Roelvink et al., 1995; Briand and Kamphuis, 1993; Zyserman and Johnson, 2002; Ding et al., 2006; Droenen and Deigaard, 2007), which determine the sediment evolution using both horizontal and vertical variations of the wave-derived parameters.

The OptiMorph model described in this paper is based on optimal control. In the past, the use of optimization theory has primarily been used in the design of coastal defense structures, whether in the design of ports and offshore breakwaters (Isebe et al., 2008; Isèbe et al., 2008).

Optimal control has already been considered for the modeling of shallow water morphodynamics, based on the assumption that the seabed acts as a flexible structure and adapts to a certain hydrodynamic quantity (Mohammadi and Bouharguane, 2011; Bouharguane et al., 2010). These studies were based on somewhat theoretical developments with no direct relationship with real case studies. Our objectives in this work is to produce a physically robust numerical morphodynamic model based on optimal control and to validate it using numerical data from well established morphodynamics software as well as wave flume experiments.

1.2. Hypotheses

OptiMorph is based on a certain number of assumptions. First, since the model is based on the minimization of a cost function, some hypotheses must be made regarding the choice of this function. This function, which originates from a physical quantity, must be directly linked to the elevation of the seabed. In the current version of the model, we set the quantity to be minimized as the energy of shoaling waves. This implies that the sea bottom reacts to the state of the waves by minimizing the energy of shoaling waves. Other assumptions assess the behavior of the sea bottom and originate from general observations. In particular, the bed-load sediment transport is controlled by the orbital displacement of water particles (Soulsby, 1987); thus a greater sediment mobility has to be considered in shallower waters. Another natural observation concerns the slope of the seabed, which cannot be overly steep without an avalanching process occurring (Reineck and Singh, 1973). Last, in an experimental wave flume, the quantity of sand must remain constant over time, with no inflow or outflow of sand to alter the sand stock.

2. Theoretical developments

2.1. Modeling framework

For the sake of simplicity, we present the principle of morphodynamics by optimization in a one-dimensional setting. This enables us to compare the numerical results based on this theory with experimental flume data. However, no assumptions are made regarding the dimension of the problem, and as a result, it is straightforward to extend this theory to a two-dimensional configuration.

We consider a coordinate system composed of a horizontal axis x and a vertical axis z. We denote $\Omega := [0, x_{\max}]$ the domain of the cross-shore profile of the active coastal zone, where $x = 0$ is a fixed point in deep water where no significant change in bottom elevation can occur, and $x_{\max}$ is an arbitrary point at the shore beyond the shoreline, as shown by Fig. 1. The elevation of the sea bottom is a one-dimensional positive function, defined by: $\psi : \Omega \times [0, T_f] \times \Psi \to \mathbb{R}^+$ where $[0, T_f]$ is the duration of the simulation (s) and Ψ is the set of physical parameters describing the characteristics of the beach profile. In order to model the evolution over time of ψ and given the assumption that ψ changes over time in response to the energy of shoaling waves, a description of the surface waves is needed.

2.2. Hydrodynamic model

The literature on hydrodynamic models is vast (Murray, 2007). However, our main focus in this work is (a) on the morphodynamic part of the approach and (b) on providing evidence of the ability of optimization to perform robust morphodynamic prediction even under weakly constrained hydrodynamics. So we present the procedures with a hydrodynamic model as simple as possible, that is based on the linear wave theory (Dean and Dalrymple, 2004), a very basic shoaling equation and some geometrical breaking parameter. It has the advantage of being easy to differentiate compared to more sophisticated models that would need automatic differentiation (Hascoet and Pascual, 2004; Mohammadi and Bouharguane, 2011) or huge additional numerical developments. This numerical implementation has a significantly short run-time as shown by the convergence results of Section 4.1. This model has the advantage of expressing wave height as an explicit function of the bottom elevation, which leads to rapid calculations of the morphodynamics.

Let h (m) be the depth of the water from a mean water level h_0 at the point where waves are generated (cf. Fig. 1). Ocean waves, here assumed monochromatic, are characterized by phase velocity C (m s^{-1}), group velocity C_g (m s^{-1}), and wave number k (m^{-1}), determined by the linear dispersion relation (1), where σ is the pulsation of the waves (s^{-1}) and g is the gravitational acceleration (m s^{-2}):

$$\sigma^2 = gk \tanh(kh) \tag{1}$$

We define Ω_S as the time-dependent subset of Ω over which the waves shoal and Ω_B the subset of Ω over which the waves break, cf. Fig. 1. Munk's breaking criterion (Munk, 1949) enables us to define $\Omega_S(t) = \left\{ x \in \Omega, \frac{H(x,t)}{h(x,t)} < \gamma \right\}$ and $\Omega_B(t) = \left\{ x \in \Omega, \frac{H(x,t)}{h(x,t)} \geq \gamma \right\}$, where γ is a wave breaking index.

Then we have:

$$H(x,t) = H_0(t) K_S(x,t) \tag{2}$$

The height of the waves H over the cross-shore profile is inspired by the shoaling Eq. (2), where $H_0(t)$ is the deep water wave height and K_S is a shoaling coefficient, given by:

$$K_S = \left(\frac{1}{2} \frac{C_0}{C_g} \right)^{\frac{1}{2}} \tag{3}$$

where C_0 is the deep water wave velocity, and:

$$n = \frac{C}{C_g}, \quad C = C_0 \tanh(kh), \quad C_g = \frac{1}{2} C \left(1 + \frac{2kh}{\sinh(2kh)} \right). \tag{4}$$

Instead of considering that waves depend solely on offshore wave height H_0, this model suggests that shoaling waves are decreasingly influenced by seawards waves. The greater the distance, the less effect it has on the present wave height. As such, we introduce a weighting function w. Assuming that the maximal distance of local spatial dependency of a wave is denoted d_w, the weighting function over the maximal distance d_w is given by $w : [0, d_w] \to \mathbb{R}^+$ such that $w(0) = 1$, $w(d_w) = 0$ and decreases exponentially.

Eq. (2) for shoaling wave height becomes Eq. (5), where H_0^w is defined by (6).

$$H(x,t) = H_0^w(x,t) K_S(x,t) \tag{5}$$

$$H_0^w(x,t) = \frac{1}{\int_{x-X}^{x} w(x-y)\mathrm{d}y} \int_{x-X}^{x} w(x-y) H(y) K(y) \mathrm{d}y \tag{6}$$

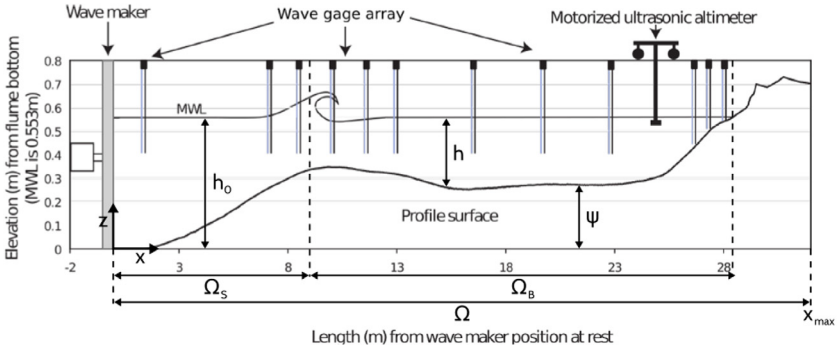

Fig. 1. Diagram of a cross-shore profile in the case of an experimental flume.

Eq. (5) applies only to the shoaling, nearshore-dependent waves of Ω_S, significant wave height over the cross-shore profile $H : \Omega \to \mathbb{R}^+$ is defined by (7), where $\alpha(x) = \frac{x}{d_w}$ over $[0, d_w]$ to allow a smooth transition between offshore and nearshore-dependent waves.

$$H(x,t) = \begin{cases} \left[(1-\alpha(x))H_0(t) + \alpha(x)H_0^w(x,t)\right] K_S(x,t) & \text{if } x \in \Omega_S \text{ and } x < d_w \\ H_0^w(x,t)K_S(x,t) & \text{if } x \in \Omega_S \text{ and } x \geq d_w \\ \gamma h(x,t) & \text{if } x \in \Omega_B \end{cases} \tag{7}$$

2.3. Morphodynamic model by wave energy minimization

The evolution of the sea bottom is assumed to be driven by the minimization of a cost function J (J s m^{-1}). Recalling the hypotheses made in Section 1.2, the shape of the beach profile is determined by the minimization of the potential energy of shoaling waves, for all $t \in [0, T_f]$:

$$J(\psi,t) = \frac{1}{16}\int_{t-T_{coupl}}^{t}\int_{\Omega_S} \rho_w g H^2(\psi,x,\tau)\mathrm{d}x\mathrm{d}\tau \tag{8}$$

where H denotes the height of the waves over the cross-shore profile (m), ρ_w is water density (kg m^{-3}), and g is the gravitational acceleration (m s^{-2}). T_{coupl} (s) defines the coupling time interval between hydrodynamic and morphodynamic models so that we have T_f/T_{coupl} iterations. In order to describe the evolution of the beach profile, whose initial state is given by ψ_0, we assume that the sea bottom elevation ψ, in its effort to minimize J, verifies the following dynamics:

$$\begin{cases} \psi_t = Y\ \Lambda\ d \\ \psi(t=0) = \psi_0 \end{cases} \tag{9}$$

where ψ_t is the evolution of the bottom elevation over time (m s^{-1}), Y is a measure of the sand mobility expressed in m s kg^{-1}, Λ measures the excitation of the seabed by the orbital motion of water waves, and d is the direction of the descent (J s m^{-2}), which indicates the manner in which the sea bottom changes. The approach involves two parameters with clear physical interpretation. The first Y takes into account the physical characteristics of the sand and represents the mobility of the sediment. Simulations with varying Y that reflect variations of the d_{50} grain diameter from 0.25 mm to 2 mm were performed. Changes in the beach profile were observed but no significant alteration of the trends in beach profile evolution through time. The asymptotic behavior of the simulations remains the same although the velocity at which a given profile is reached changes. Further explanation of the nature of the Y parameter will be given at a later stage of the model development. The second parameter Λ is a local function which represents the influence of the relative water depth kh on the beach profile dynamics and is defined after the term describing the vertical attenuation of the velocity potential according to linear wave theory (Soulsby, 1987):

$$\begin{array}{rccc} \Lambda: & \Omega \times [0,h_0] & \longrightarrow & \mathbb{R}^+ \\ & (x,z) & \longmapsto & \dfrac{\cosh(k(x)(h(x)-(h_0-z)))}{\cosh(k(x)h(x))} \end{array} \tag{10}$$

In unconstrained circumstances, for instance, if a total sand volume constraint does not need to be enforced, we set $d = -\nabla_\psi J$, which indicates a direction for local minimization of J with regards to ψ. The calculation of $\nabla_\psi J$ is described in Appendix A.1. However, constraints are added to the model to incorporate more physics and to deliver more realistic results. While driving forces behind the morphological evolution of the beach profile are described by the minimization of the cost function J, secondary processes are expressed by constraints. In the interest of simplicity, we have adopted two physical constraints though more can be introduced if necessary. The first concerns the local slope of the bottom. Depending on the composition of the sediment, the bottom slope is bounded by a grain-dependent threshold M_{slope} (Dean and Dalrymple, 2004). This is conveyed by the following constraint on the local bottom slope:

$$\left|\frac{\partial\psi}{\partial x}\right| \leq M_{\text{slope}} \tag{11}$$

The dimensionless parameter M_{slope} represents the critical angle of repose of the sediment. This angle is based on observed angles in natural beach environments, which are often between 0.01 and 0.2 (Bascom, 1951; Vos et al., 2020; Short, 1996). We have considered the observed critical angle of 0.2.

A second example concerns the sand stock in the case of an experimental flume. In a flume, the quantity of sand must be constant over time, as given by (12), contrarily to an open-sea configuration where sand can be transported between the nearshore zone and a domain beyond the closure water depth where sediment is lost definitely for beach morphodynamics (Hattori and Kawamata, 1980; Quick, 1991). This constraint can be written as :

$$\int_\Omega \psi(t,x)\mathrm{d}x = \int_\Omega \psi_0(x)\mathrm{d}x \qquad \forall t \in [0,T_f] \tag{12}$$

This constraint is necessary for verifying and validating the numerical model with the wave flume experimental data.

3. Numerical application

In this section, we present the numerical results produced by the OptiMorph model. For validation purposes, the resulting beach profile is compared to experimental data acquired during a flume experiment. We also conduct a comparative analysis between the beach profiles produced experimentally, by OptiMorph and by XBeach, with

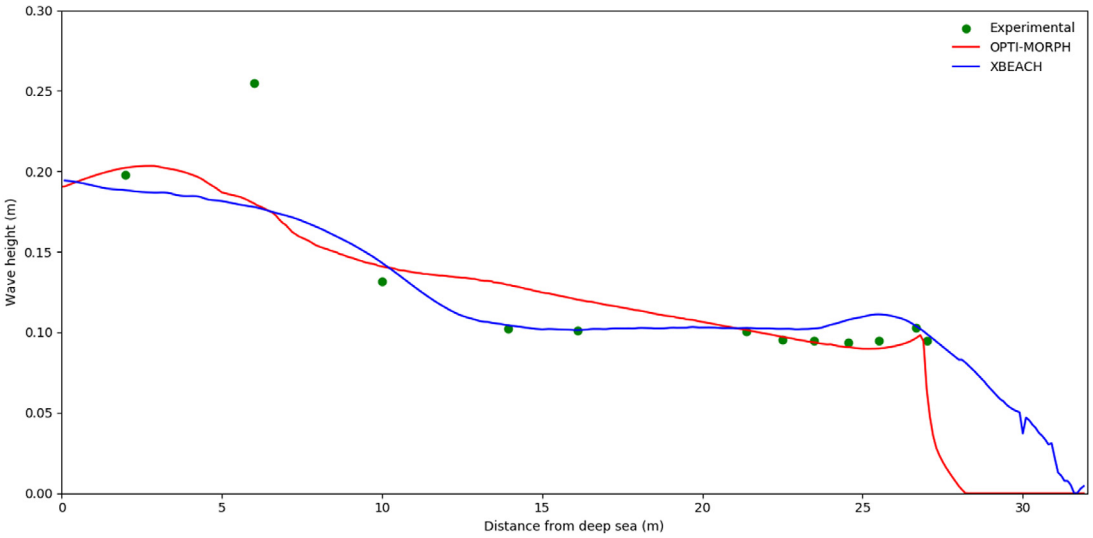

Fig. 2. Comparison of mean wave height over a storm simulation. The green points correspond to the mean wave height provided by the gauges of the flume experiment. The mean wave height determined by OptiMorph (red) and XBeach (blue) also appears. The non-zero wave height beyond the shoreline as presented by XBeach is due to wave set-up, which OptiMorph does not handle.

the aim of assessing how OptiMorph holds up against existing hydro-morphodynamic models. A brief description of the experiment is provided, as well the XBeach model.

3.1. Description of the experiment

The experimental observations have been collected as part of the COPTER project and a series of laboratory wave-flume experiments were performed in order to investigate the morphodynamic impact of introducing solid geotextile tubes in the nearshore (Bouchette, 2017). We use the part of the experiment run without tubes that was devoted to the description of the natural evolution of the beach profile under various wave conditions. Time and length scale ratio are set to $1/3$ and $1/10$ respectively to that of the field.

A flume measuring 36 m long, 0.55 m wide and 1.3 m deep is equipped with a wave-maker and gauges measuring the elevation of the water surface from which wave properties are derived. Artificial particles are placed inside the flume representing the mobile sea bottom and an ultrasonic gauge is used to measure the experimental beach profile. The experimental beach profile, described in Fig. 1 is subjected to a series of 30-minute storm climates, among which a typical moderate storm event (at the scale of the flume) with a significant wave height and period of $H_s = 135$ mm and $T_s = 2.5$ s.

3.2. Xbeach model

XBeach is an open-source process-based model developed by Deltares, UNESCO-IHE, and Delft University of Technology to simulate the hydro-morphodynamic processes in coastal areas (Roelvink et al., 2009; Zimmermann et al., 2012; Bugajny et al., 2013; Williams et al., 2015). In brief, XBeach uses four interconnected modules to model near-shore processes (Daly, 2009; Roelvink et al., 2010). The two hydrodynamic modules consist of the short wave module and the flow module. The first is based on wave action equations (Holthuijsen et al., 1989), and incorporates breaking, dissipation (Roelvink, 1993), and wave current interactions, while the latter is governed by shallow water equations (Andrews and Mcintyre, 1978; Walstra et al., 2000). One of the two morphodynamic modules is the sediment transport module based on the equilibrium sediment concentration equation (Soulsby, 1997) and a depth-averaged advection–diffusion equation (Galappatti and Vreugdenhil, 1985). The other is the morphology module which concerns seabed transformations such as the evolution of the sea bottom and avalanching.

For the simulations, the domain Ω is defined over 32 m with a uniform subdivision of 320 cells. The incoming wave boundary condition is provided using a JONSWAP wave spectrum (Hasselmann et al., 1973), with a significant wave height of $H_{m0} = 0.015$ m and a peak frequency at $f_p = 0.4$ s^{-1}. The breaker model uses the Roelvink formulation (Roelvink, 1993), with a breaker coefficient of $\gamma = 0.4$, a power $n = 15$, and a wave dissipation coefficient of 0.5. These parameters were calibrated using the hydrodynamic data produced during the physical flume experiment. Concerning sediment parameters, the d_{50} coefficient is set as 0.0006, and the porosity is 2650 kg m^{-3}. No other parameters such as bed friction or vegetation were applied. The model is set to run for a period of 1800 s, as a short-term simulation.

3.3. Hydrodynamic validation

This section is devoted to the comparison of the two numerical hydrodynamic models to the experimental wave data obtained in the experimental flume of Section 3.1. Mean wave height profiles were calculated over the short-term storm simulation, for both OptiMorph and XBeach, and compared to the mean wave height of the experimental model. The latter was calculated using the measures taken by the gauges of the flume.

Fig. 2 shows that the hydrodynamic module of both OptiMorph (red) and XBeach (blue) are both comparable with respect to the experimental measurements (green) excluding, as is often the case, the second point at $x = 6$ m. XBeach demonstrates a close qualitative fit over the 10–22 m section of the flume, whereas OptiMorph excels at the coast (21–27 m), with a near-perfect fit with the experimental data. Despite the simplicity of the hydrodynamic model used by OptiMorph, the resulting wave height is of the same order of magnitude over the cross-shore profile than that measured during the flume experiment, which indicates that the resulting beach profile would be comparable with regard to the forcing energy driving the morphodynamic response.

3.4. Numerical results of the morphodynamic simulations

The OptiMorph model was applied to the configuration of the COPTER experiment of Section 3.1, and the resulting beach profile

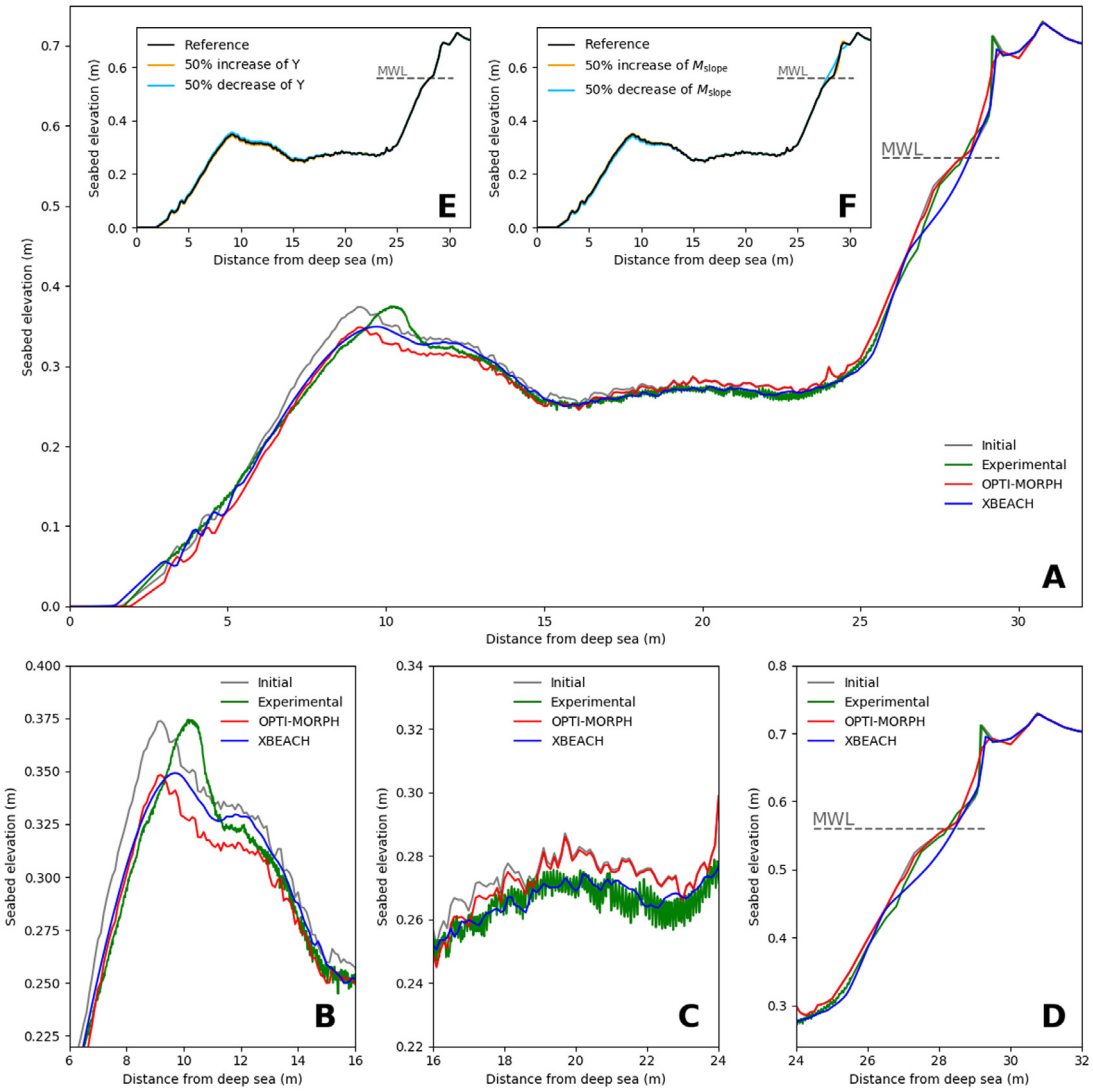

Fig. 3. A. Results of the numerical simulation calculated over the initial seabed (gray) using the XBeach morphodynamic module (blue) and the OptiMorph model (red). These are compared with the experimental data acquired during the COPTER project (green). The mean water level is denoted MWL and is set at 0.56 m. **B.** Zoomed in view of the sandbar, located between 6 m and 16 m. **C.** Zoomed in view of the plateau, located between 16 m and 24 m. **D.** Zoomed in view at the shoreline, located between 24 m and 32 m. **E.** Robustness analysis of the mobility parameter Y. The reference profile is depicted in black. The orange (resp. light blue) profile is the result of a 50% increase (resp. decrease) in mobility, with all other parameters remaining the same. **F.** Robustness analysis of the maximal sand slope parameter M_{slope}. The reference profile is depicted in black. The orange (resp. light blue) profile is the result of a 50% increase (resp. decrease) of M_{slope}, with all other parameters remaining the same.

is shown by the red profile, in Fig. 3.A. The main observation is the decrease of 2.5 cm in height of the sandbar, at $x = 9$ m. We observe a slight lowering of the sea bottom adjacent to the wave-maker, and a slight increase at the plateau, situated at 15–25 m. No mobility is observed at the coast.

When comparing the results provided by OptiMorph (red), with that of XBeach (blue) and the experimental data (green), as shown on Fig. 3.A, we observe that the red beach profile provided by the OptiMorph model shows a general quantitative agreement when compared to the experimental data, as does the XBeach morphological module. In fact, both models produce profiles close to the experimental data over the plateau located at 15–25 m from the wave-maker (Fig. 3.C). At the shore, OptiMorph matches the experimental data whereas XBeach shows a vertically difference of up to 3 cm at $x = 27$ m (Fig. 3.D). Discrepancies on the part of both models occur in the area surrounding the tip of the sandbar, as both OptiMorph and XBeach fail to predict the shoreward shift of the sandbar (Fig. 3.B); the experimental data show that the height of the sandbar remains unchanged with regards to the initial profile. Both sandbars have a height of 0.375 m; however, the sandbar resulting from the experimental simulation has moved towards the coast, an occurrence that neither numerical model was able to predict.

As such, this new model based on wave-energy minimization shows potential when compared to XBeach, in the case of short-term simulations.

4. Discussion

4.1. Robustness analysis of the convergence in time and space of the hydrodynamic model

We computed a reference OptiMorph simulation using a very small coupling time of 0.05 s which is much smaller than what is usually used in hydro-morphodynamic simulations. The simulation was performed with the original bathymetric profile of the COPTER experiment and the forcings of the wave maker.

This simulation provides a reference computed sea bed $\psi_{ref}(T_f, x)$ at some given time T_f. We would like to see the convergence toward this reference solution of various other OptiMorph simulations with

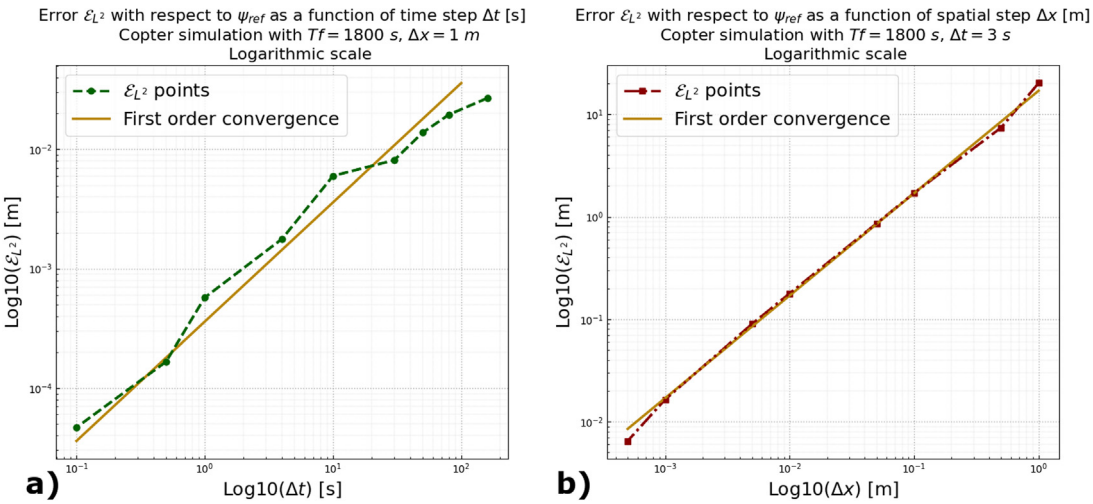

Fig. 4. (a) Errors $\mathcal{E}_{L^2}$ (green) obtained by simulations of 10 different time steps compared to the reference simulation corresponding to a coupling time of 0.05 s. First order convergence (yellow). (b) Errors $\mathcal{E}_{L^2}$ (red) obtained by simulations of 10 different spatial steps compared to the reference simulation corresponding to a spatial step of 0.0002 m. First order convergence (yellow).

different decreasing time steps. From this series of simulations, we quantify a residual error with L^2 norm as $\mathcal{E}_{L^2} = \|\psi_{ref} - \psi\|_{L^2}$ in m. We performed 10 simulations with time steps ranging in $[0.05; 160]$ s and we get the results described in Fig. 4.(a).

In order to analyze the convergences in space and time, we choose, respectively, a reference coupling time of $T_{coupl} = 3$ s and a spatial step size $\Delta x = 1$ m. $T_{coupl} = 3$ s corresponds to the kind of time steps we would like to use in simulations. But, we will use larger spatial resolution in practice. The results in Fig. 4 show first order (illustrated by the continuous line) convergence rates in both time and space.

To understand why a coupling time of 3 s is interesting for computing efficiency, it is useful to look at the CFL stability condition analysis for the shallow-water Saint-Venant model. The analysis provides a typical upper bound for the time step of the form:

$$\Delta t = \min_i \left(\frac{\Delta x}{2 \max_i(|u_i \pm \sqrt{g h_i}|)} \right) = \frac{\Delta x}{2 \max_i(|u_0 \pm \sqrt{g h_0}|)},$$

where subscript i indicates the mesh node which means that the minimum is taken over all the nodes of the mesh. In our situation, it correspond to the off-shore position (subscript $i = 0$). Typical values in our simulation are: $u_0 = 10$ m s^{-1}, $\Delta x = 1$ m, $h = 0.55$ m and $g = 9.81$ m s^{-2}. This gives us $\Delta t = 0.04$ s, which is about two orders of magnitude smaller than our reference time step of $\Delta t = 3$ s. In addition, the costs of one iteration of the Saint-Venant and OptiMorph models are comparable.

4.2. Parameter robustness analysis

One of the advantages of the OptiMorph model is the low number of morphodynamic hyper-parameters required. At the present time, OptiMorph requires two hyper-parameters: the mobility parameter Υ and the maximal slope parameter M_{slope}. Here, an assessment on these parameters is conducted. In Fig. 3.E, three simulations were performed in identical settings with changes made solely to the mobility parameter. Initially, this parameter Υ has a value of 5×10^{-6} m s kg^{-1}. Fig. 3.E shows no significant difference despite a 50% increase ($\Upsilon = 7.5 \times 10^{-6}$ m s kg^{-1}) (orange) or decrease ($\Upsilon = 2.5 \times 10^{-6}$ m s kg^{-1}) (light blue) of Υ with regard to the baseline beach profile (black). Similar conclusion can be deduced for the maximal slope parameter M_{slope}, whose reference value here is 0.2. The corresponding parameter of XBeach is *wetslp*, described in the XBeach manual as the critical avalanching slope under water, and is also set to 0.2. In Fig. 3.F, we observe little difference between the reference seabed (black), the seabed resulting from a 50% increase ($M_{\text{slope}} = 0.3$) (orange) and the seabed resulting from a 50% decrease ($M_{\text{slope}} = 0.1$) (light blue). The only apparent discrepancy can be found at $x = 28$ m, where the bottom slope is at its steepest, and therefore the sand slope constraint is more prone to be active. The reduction of the critical angle of repose results naturally in a less steep slope. The robustness of OptiMorph in relation to both the mobility parameter and the slope parameter, despite a significant increase or decrease of their value, is apparent. Further simulations show that the robustness of these parameters is not specific to this particular flume configuration, but can be observed regardless of the initial configuration.

4.3. Mid-term simulations

This section is devoted to a medium term behavior of OptiMorph, the main question being, is this numerical model capable of creating an equilibrium state after being subjected to a great number of repeated events. Five forcing scenarios, lasting either 2 or 6 days, were applied to the same initial seabed in the same parametric configuration. The current OptiMorph code is in Python. Typically, using time-steps of 1 s simulating a day of forcing requires about 1.5 h on a 2 GHz PC computer. Each time iteration gathering the steps presented in this paper requires therefore about 63 ms. Regarding Section 4.1, we could use 3 s time-step and divide the simulation time by 3. An analysis of the resulting beach profiles is performed as well as their behavior throughout the simulation. The latter is achieved through a comparative study of four time-series, focusing on: (1), the vertical evolution of bottom elevation at the tip of the sandbar; (2), the vertical evolution of bottom elevation at a point of the plateau; (3), the distance between the wavemaker and the onset of the sea bottom; and (4), the location of the shoreline position.

Applying OptiMorph over a longer time-series leads to the results of Fig. 5. The two 2-day forcing scenarios are shown in Fig. 5.A and B. In both cases, we observe that the resulting beach profiles in Fig. 5.F are subjected to the destruction of the sandbar and have a tendency

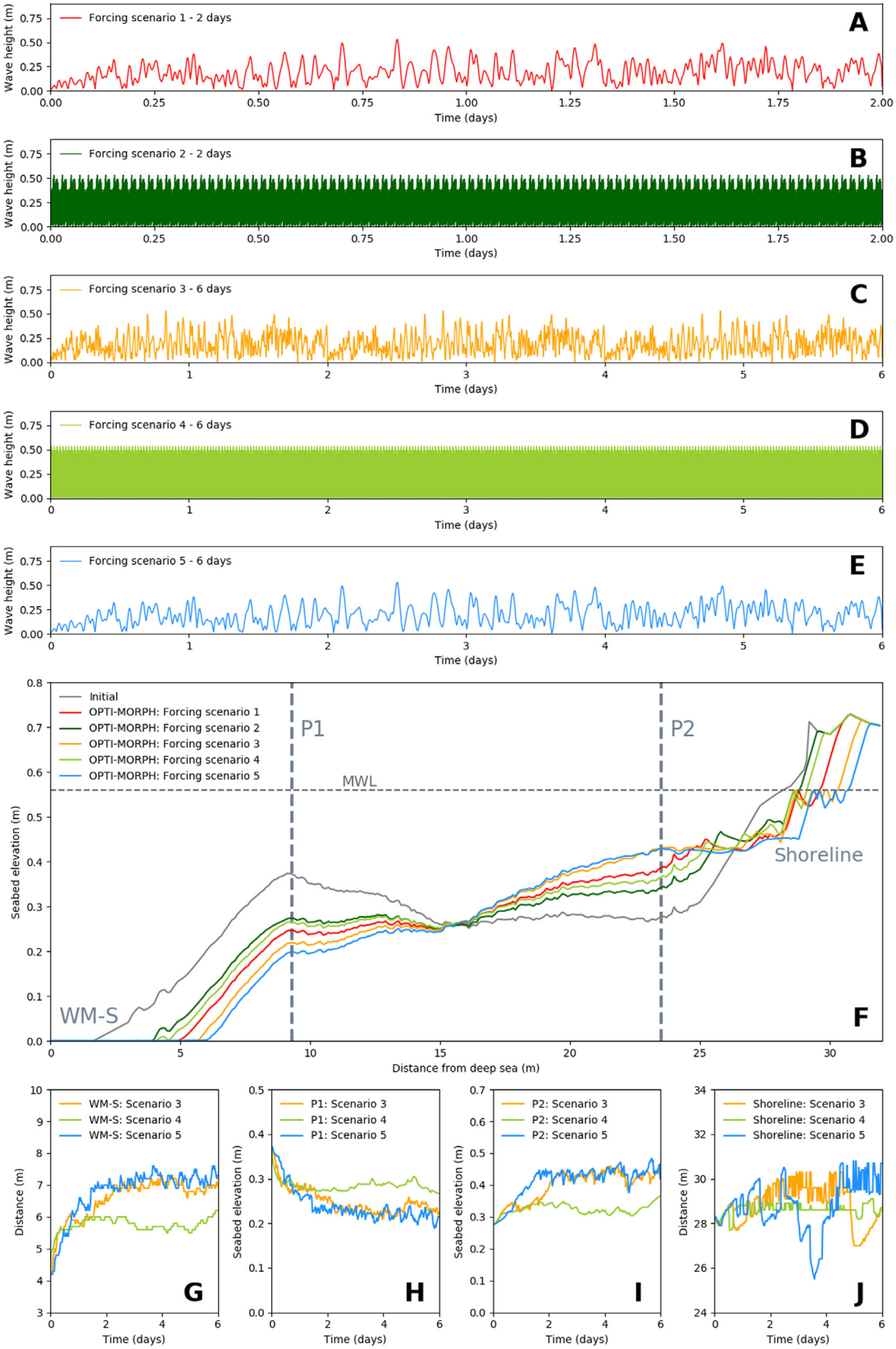

Fig. 5. Mid-term simulation of OptiMorph. **A.** Forcing wave height for scenario 1, composed of several mid-term events over a 2-day period. **B.** Forcing wave height for scenario 2, composed of numerous short-term events over a 2-day period. **C.** Forcing wave height for scenario 3, composed of several mid-term events over a 6-day period. **D.** Forcing wave height for scenario 4, composed of numerous short-term events over a 6-day period. **E.** Forcing wave height for scenario 5, composed of few mid-term events over a 6-day period. **F.** Seabeds resulting from the different forcing scenarios produced by OptiMorph. Two points of interest have be identified: P1 located at $x = 9.3$ m and P2 located at $x = 20.1$ m. **G.** Evolution of the distance, devoid of sediment, between the wave-maker (located at $x = 0$ m) and the seabed (WM-S), regarding forcing scenarios 3, 4, and 5. **H.** Vertical evolution of seabed elevation at P1, driven by the 6-day forcing scenarios 3, 4, and 5. **I.** Vertical evolution of seabed elevation at P2, driven by the 6-day forcing scenarios 3, 4, and 5. **J.** Evolution of shoreline position, driven by the 6-day forcing scenarios 3, 4, and 5.

to evolve progressively towards an equilibrium beach profile (U.S. Army Corps of Engineers, 2002). Simulations over a 6-day period were conducted to confirm this tendency. These scenarios are depicted in Fig. 5.C, D, and E; the resulting profiles given in Fig. 5.F show once again the destruction of the sandbar, the elevation of the plateau, and some erosion at the shoreline. Furthermore, all three tend towards an equilibrium state. This is confirmed by the four time-series analysis presented in Fig. 5.G, H, I, and J. The vertical elevation of the seabed at both points P1 and P2 show initial variations over the first 2 days: a decrease in the case of P1 (cf. Fig. 5.H) and an increase in the case of P2 (cf. Fig. 5.I). However, both studies show a stabilization of the sea bottom elevation over the last 4 days of the 6-day period. Similar conclusions can be drawn regarding the length of the zone containing no sediment adjacent to the wave-maker (cf. Fig. 5.G). An initial increase between 2 and 3 meters can be observed, with stability achieved in the later stages of the simulations. Finally, Fig. 5.J shows the evolution of the shoreline position. Initially found at $x = 28.3$ m, all scenarios provoke a retreat of the shoreline: 0.4 m in scenario 3, 0.3 m in scenario 4, and 2 m in scenario 5. The shorelines of the latter two converge, whereas scenario 3 shows an abrupt advance of the shoreline at day 5, with an attempt to return back to its stable state of $x = 30$ m. The seabed has been flattened, the sandbar has been destroyed and erosion can be observed at the coast (Grasso et al., 2011). This tendency to evolve towards an equilibrium state (Dean and Dalrymple, 2004) is consistent with the choice of morphogenic and constant storm-like forcing conditions.

The comparisons made between the two 2-day simulations and the three 6-day simulations, in this quite limited configuration, also reveal the little influence heritage has on the morphodynamic response. Both scenarios 1 and 2 have a comparable cumulative incoming wave energy density $E = \frac{1}{16}\int_0^T \rho g H_0^2 \mathrm{d}t$ of 0.0591 J m^{-2}. The resulting beach profiles evolve towards similar profiles (reduction of the sandbar, increase of elevation of the plateau, and erosion at the coast), despite two different forcing conditions. Similar conclusions can be drawn regarding the 6-day simulations, where the cumulative energy density of all three is equal to 0.177 J m^{-2}.

5. Conclusions

OptiMorph shows potential as a fast, robust, and low complexity morphodynamic model involving only two hyper-parameters. Despite using a basic hydrodynamic model for the description of the complex coupling of hydrodynamic and morphodynamic processes, we can nevertheless observe that a numerical model based on an optimization theory works effectively, with comparable results to a state of the art hydro-morphodynamic model requiring the tuning of dozens of hyper-parameters. Mid-term simulations also show typical morphodynamic behavior, with the tendency of the seabed to evolve towards an equilibrium state. These results demonstrate the tremendous potential of OptiMorph, a constrained energy minimization morphodynamic model.

Declaration of competing interest

The authors declare that they have no known competing financial interests or personal relationships that could have appeared to influence the work reported in this paper.

Data availability

Data will be made available on request.

Acknowledgments

This work was conducted as part as M. Cook's PhD studies which is funded by BRLi and M. Dupont's PhD studies which is funded by the CNRS. We are grateful to BRLi for their assistance throughout the development of preliminary versions of the morphodynamic model by optimization. We thank also the GLADYS network (www.gladys-littoral.org) for its continuous logistical and financial support of academic research and applications on coastal hydrodynamics in the South of France. The COPTER experiment was conducted in the framework of project ANR Blanche 2005–006. The development of OptiMorph has been made possible thanks to european funds in the framework of OPTIBEACH project and CNRS, France funds in the framework of the french MITI program.

Appendix. Mathematical developments

In this section, we detail some of the mathematical results needed in the implementation of the OptiMorph model, specifically the calculation of the gradient of the cost function J (Eq. (8)) with regard to the sea bottom elevation ψ, which in turn requires the gradient of the wave height function (Eq. (7)) with regard to ψ. With the current choice of hydrodynamic model, this can be achieved analytically. With more sophisticated hydrodynamic models this is not always possible. In these cases, if the source code of the model is available, the calculation of the gradient can be performed using automatic differentiation of programs (Griewank and Walther, 2008; Hascoet and Pascual, 2004) directly providing a computer program for the gradient.

A.1. Gradient of the cost function with respect to sea bottom elevation

OptiMorph requires the evaluation of gradient of the functional J with respect to the sea bottom elevation ψ, denoted $\nabla_\psi J$. For our functional of the form $J(H(\psi(x)))$ involving dependencies with respect to hydrodynamic quantities H, this sensitivity is given by:

$$\nabla_\psi J = \nabla_H J \, \nabla_\psi H. \tag{A.1}$$

$\nabla_\psi H$ requires the linearization of the hydrodynamic model, and ψ is a parametric representation of the bathymetry.

A.2. Gradient of the wave height with respect to the sea bottom elevation

This section is devoted to the calculation of the gradient of the wave height H, given by (7), with regards to the sea bottom elevation ψ and denoted $\nabla_\psi H$. Being as $h = h_0 - \psi$, the derivation of the third line of (7) with regards to ψ is immediate. The calculation of the gradient of the first line of (7) is analogous to that of the second. It remains to differentiate the second line of (7) with regards to ψ. Observing that the chain rule yields for all $x, t \in \Omega_S \times [0, T_f]$ with $x \geq d_w$,

$$\nabla_\psi H(x,t) = H_0^w(x,t)\nabla_\psi K_S(x,t) + \nabla_\psi H_0^w(x,t) K_S(x,t), \tag{A.2}$$

and that the term $\nabla_\psi H_0^w(x,t)$ can be determined iteratively, using $\nabla_\psi H_0 = 0$, it remains to determine $\nabla_\psi K_S(x,t)$. Injecting the definitions of n, C and C_g, given in (4), yields

$$K_S = \left[\tanh(kh)\left(1 + \frac{2kh}{\sinh(2kh)}\right)\right]^{-1/2}. \tag{A.3}$$

For the sake of simplicity, let $U = \tanh(kh)\left(1 + \frac{2kh}{\sinh(2kh)}\right)$ and $X = kh$. Eq. (A.3) becomes

$$\nabla_\psi K_S = -\frac{1}{2}\, U^{-3/2}\, \nabla_\psi U, \tag{A.4}$$

and we have

$$\nabla_\psi U = \nabla_\psi X \frac{2\cosh^2(X) - X\sinh(2X)}{\cosh^4(X)}, \tag{A.5}$$

with $\nabla_\psi X = h\nabla_\psi k + k\nabla_\psi h = h\nabla_\psi k - k$. Moreover, differentiating both sides of the dispersion Eq. (1) by ψ gives

$$\nabla_\psi k = \frac{k^2}{\cosh(kh)\sinh(kh) + kh}. \tag{A.6}$$

Combining (A.4),(A.5), and (A.6), we obtain $\nabla_\psi K_S$, and therefore $\nabla_\psi H$.

References

Andrews, D.G., Mcintyre, M.E., 1978. An exact theory of nonlinear waves on a Lagrangian-mean flow. J. Fluid Mech. 89 (4), 609–646. http://dx.doi.org/10.1017/S0022112078002773.

Bascom, W.N., 1951. The relationship between sand size and beach-face slope. EOS Trans. Am. Geophys. Union 32 (6), 866–874.

Bouchette, F., 2017. Coastal defense strategy along hatzuk beach (northern tel aviv, israel). insights from the copter physical experimentation with moveable bed. Technical Report 17-1, BRL Ingénierie, Nîmes.

Bouharguane, A., Azerad, P., Bouchette, F., Marche, F., Mohammadi, B., 2010. Institut de mathématiques et de Modélisation de monptellier, université Montpellier II, 34 095 montpellier low complexity shape optimization & a posteriori high fidelity validation. Discrete Contin. Dyn. Syst. - B 13 (4), 759–772. http://dx.doi.org/10.3934/dcdsb.2010.13.759, URL http://aimsciences.org//article/doi/10.3934/dcdsb.2010.13.759.

Bouharguane, A., Mohammadi, B., 2012. Minimization principles for the evolution of a soft sea bed interacting with a shallow. Int. J. Comput. Fluid Dyn. 26, 163–172. http://dx.doi.org/10.1080/10618562.2012.669831.

Briand, M.-H., Kamphuis, J., 1993. Sediment transport in the surf zone: A quasi 3-D numerical model. Coast. Eng. 20, 135–156. http://dx.doi.org/10.1016/0378-3839(93)90058-G.

Bruun, P., 1954. Coast Erosion and the Development of Beach Profiles. In: Technical memorandum - Beach Erosion Board ;no. 44, U.S. Beach Erosion Board, [Washington], pp. 78–79, URL http://hdl.handle.net/2027/uiug.30112088627325, Bibliography,

Bugajny, N., Furmanczyk, K., Dudzinska-Nowak, J., Paplińska-Swerpel, B., 2013. Modelling morphological changes of beach and dune induced by storm on the southern baltic coast using XBeach (case study: Dziwnow spit). J. Coast. Res. I, 672–677. http://dx.doi.org/10.2112/SI65-114.1.

Coeffe, Y., Pechon, P., 1982. Modelling of sea-bed evolution under waves action. In: Proc. 18th ICCE, Vol. 1. http://dx.doi.org/10.9753/icce.v18.71.

Cook, M., Bouchette, F., Mohammadi, B., Sprunck, L., Fraysse, N., 2021. Optimal Port Design Minimizing Standing Waves with A Posteriori Long Term Shoreline Sustainability Analysis. China Ocean Engineering 35, 802–813.

Daly, C., 2009. Low frequency waves in the shoaling and nearshore zone a validation of xbeach. In: Erasmus Mundus Master in Coastal and Marine Engineering and Management (CoMEM). Delft University of Technology.

Dean, R., Dalrymple, R., 2004. Coastal processes with engineering applications. In: Coastal Processes with Engineering Applications, By Robert G. Dean and Robert A. Dalrymple. Cambridge University Press, Cambridge, UK, ISBN: 0521602750, p. 487.

Ding, Y., Wang, S., Jia, Y., 2006. Development and validation of a quasi-three-Dimensional Coastal Area morphological model. J. Waterway Port Coast. Ocean Eng. 132, 462–476. http://dx.doi.org/10.1061/(ASCE)0733-950X(2006)132:6(462).

Droenen, N., Deigaard, R., 2007. Quasi-three-dimensional modelling of the morphology of longshore bars. Coast. Eng. 54, 197–215. http://dx.doi.org/10.1016/j.coastaleng.2006.08.011.

Fleming, C., Hunt, J., 1977. Application of sediment transport model. pp. 1184–1202. http://dx.doi.org/10.1061/9780872620834.070.

Galappatti, G., Vreugdenhil, C., 1985. A depth-integrated model for suspended sediment transport. J. Hydraul. Res. 23 (4), 359–377.

Grasso, F., Michallet, H., Barthélemy, E., 2011. Experimental simulation of shoreface nourishments under storm events: A morphological, hydrodynamic, and sediment grain size analysis. Coast. Eng. 58 (2), 184–193. http://dx.doi.org/10.1016/j.coastaleng.2010.09.007.

Gravens, M., 1997. An approach to modeling inlet and beach evolution. pp. 4477–4490. http://dx.doi.org/10.1061/9780784402429.348.

Griewank, A., Walther, A., 2008. Evaluating Derivatives: Principles and Techniques of Algorithmic Differentiation, second ed. Society for Industrial and Applied Mathematics, http://dx.doi.org/10.1137/1.9780898717761.

Hascoet, L., Pascual, V., 2004. Tapenade user's guide. In: INRIA Technical Report. INRIA, pp. 1–31.

Hasselmann, K., Barnett, T., Bouws, E., Carlson, H., Cartwright, D., Enke, K., Ewing, J., Gienapp, H., Hasselmann, D., Kruseman, P., Meerburg, A., Muller, P., Olbers, D., Richren, K., Sell, W., Walden, H., 1973. Measurements of Wind-Wave Growth and Swell Decay During the Joint North Sea Wave Project (JONSWAP). Technical report, Deutsches Hydrographisches Institut, Hamburg, Germany, pp. 1–95.

Hattori, M., Kawamata, R., 1980. Onshore-offshore transport and beach profile change. pp. 1175–1193. http://dx.doi.org/10.1061/9780872622647.072.

Holthuijsen, L., Booij, N., Herbers, T., 1989. "A prediction model for stationary, short crested waves in shallow water with ambient current". Coast. Eng. 13, 23–54. http://dx.doi.org/10.1016/0378-3839(89)90031-8.

Isèbe, D., Azerad, P., Bouchette, F., Ivorra, B., Mohammadi, B., 2008. Shape optimization of geotextile tubes for sandy beach protection. Int. J. Numer. Methods Eng. 74 (8), 1262–1277. http://dx.doi.org/10.1002/nme.2209.

Isèbe, D., Azérad, P., Bouchette, F., Mohammadi, B., 2014. Design of passive defense structures in coastal engineering. International Review of Civil Engineering (IRECE) 5 (2), http://dx.doi.org/10.15866/irece.v5i2.2029.

Isebe, D., Azerad, P., Mohammadi, B., Bouchette, F., 2008. Optimal shape design of defense structures for minimizing short wave impact. Coast. Eng. 55 (1), 35–46. http://dx.doi.org/10.1016/j.coastaleng.2007.06.006.

Johnson, H., Brøker, I., Zyserman, J., 1995. Identification of some relevant processes in coastal morphological modelling. pp. 2871–2885. http://dx.doi.org/10.1061/9780784400890.208.

Kana, T., Hayter, E., Work, P., 1999. Mesoscale sediment transport at southeastern U.S. tidal inlets: conceptual model applicable to mixed energy settings. J. Coast. Res. 15, 303–313.

Larson, M., Kraus, N., 1989. Numerical Model for Simulating Storm- Induced Beach Change. Report 1. Empirical Foundation and Model Development. Technical report, Department of the Army US Army Corps of Engineers, Washington, DC, USA, p. 266.

Larson, M., Kraus, N., Byrnes, M., 1990. Numerical Model for Simulating Storm-Induced Beach Change. Report 2. Numerical Formulation and Model Tests. Technical report, Department of the Army US Army Corps of Engineers, Washington, DC, USA, p. 120.

Latteux, B., 1980. Harbour design including sedimentological problems using mainly numerical technics. pp. 2213–2229. http://dx.doi.org/10.1061/9780872622647.133.

Lesser, G., Roelvink, D.J., Kester, J., Stelling, G., 2004. Development and validation of a three-dimensional morphological model. Coast. Eng. 51, 883–915. http://dx.doi.org/10.1016/j.coastaleng.2004.07.014.

Maruyama, K., Takagi, T., 1988. A simulation system of near-shore sediment transport for the coupling of the sea-bottom topography, waves and currents. In: Proc. IAHR Symp. Math. Mod. Sed. Transp. Coastal Zone. pp. 300–309.

McCarroll, R.J., Masselink, G., Valiente, N.G., Scott, T., Wiggins, M., Kirby, J.-A., Davidson, M., 2021. A rules-based shoreface translation and sediment budgeting tool for estimating coastal change: ShoreTrans. Mar. Geol. 435, 106466. http://dx.doi.org/10.1016/j.margeo.2021.106466.

Mohammadi, B., 2017. Uncertainty quantification in littoral erosion. Comput. & Fluids 143, 120–133. http://dx.doi.org/10.1016/j.compfluid.2016.10.017.

Mohammadi, B., Bouchette, F., 2014. Extreme scenarios for the evolution of a soft bed interacting with a fluid using the value at risk of the bed characteristics. Comput. & Fluids 89, 78–87. http://dx.doi.org/10.1016/j.compfluid.2013.10.021.

Mohammadi, B., Bouharguane, A., 2011. Optimal dynamics of soft shapes in shallow waters. Comput. & Fluids 40, 291–298. http://dx.doi.org/10.1016/j.compfluid.2010.09.031.

Munk, W., 1949. The solitary wave theory and its application to surf problems. Ann. New York Acad. Sci. 51, 376–424. http://dx.doi.org/10.1111/j.1749-6632.1949.tb27281.x.

Murray, A.B., 2007. Reducing model complexity for explanation and prediction. Geomorphology 90 (3), 178–191. http://dx.doi.org/10.1016/j.geomorph.2006.10.020, Reduced-Complexity Geomorphological Modelling for River and Catchment Management.

Nairn, R., Southgate, H., 1993. Deterministic profile modelling of nearshore processes. Part 2. sediment transport and beach profile development. Coast. Eng. 19, 57–96. http://dx.doi.org/10.1016/0378-3839(93)90019-5.

Nicholson, J., Brøker, I., Roelvink, D.J., Price, D., Tanguy, J.-M., Moreno, L., 1997. Intercomparison of coastal area morphodynamic models. Coast. Eng. - COAST. ENG. 31, 97–123. http://dx.doi.org/10.1016/S0378-3839(96)00054-3.

Quick, M., 1991. Onshore-offshore sediment transport on beaches. Coast. Eng. 15, 313–332.

Reineck, H.-E., Singh, I.B., 1973. In: Reineck, H.-E., Singh, I.B. (Eds.), Depositional Sedimentary Environments; with Reference To Terrigenous Clastics.

Roelvink, D.J., 1993. Dissipation in random wave groups incident on a beach. Coast. Eng. - COAST. ENG. 19, 127–150. http://dx.doi.org/10.1016/0378-3839(93)90021-Y.

Roelvink, D.J., Reniers, A., van Dongeren, A., Thiel de Vries, J., Lescinski, J., McCall, R., 2010. XBeach Model – Description and Manual. Technical report, Unesco-IHE Institute for Water Education, Deltares and Delft University of Technology, Delft, Netherlands.

Roelvink, D.J., Reniers, A., van Dongeren, A., Thiel de Vries, J., McCall, R., Lescinski, J., 2009. Modelling storm impacts on beaches, dunes and barrier islands. Coast. Eng. 56, 1133–1152. http://dx.doi.org/10.1016/j.coastaleng.2009.08.006.

Roelvink, J.A., Van Banning, G.K.F.M., Verwey, A., 1994. Design and development of DELFT3D and application to coastal morphodynamics, 1st international conference, hydroinformatics 94. In: Hydroinformatics 94, HYDROINFORMATICS -PROCEEDINGS-, 1st International Conference, Hydroinformatics 94, Vol. 1. International Association for Hydraulic Research, Balkema, Rotterdam, pp. 451–456.

Roelvink, D.J., Walstra, D.-J., Chen, Z., 1995. Morphological modelling of Keta Lagoon case. pp. 3223–3236. http://dx.doi.org/10.1061/9780784400890.233.

Ruessink, G., Terwindt, J., 2000. The behaviour of nearshore bars on the time scale of years: A conceptual model. Mar. Geol. 163, 289–302. http://dx.doi.org/10.1016/S0025-3227(99)00094-8.

Short, A.D., 1996. The role of wave height, period, slope, tide range and embaymentisation in beach classifications: A review. Revis. Chil. Hist. Nat. 69, 589–604.

Soulsby, R., 1987. Calculating bottom orbital velocity beneath waves. Coast. Eng. - COAST. ENG. 11, 371–380. http://dx.doi.org/10.1016/0378-3839(87)90034-2.

Soulsby, R., 1997. Dynamics of Marine Sands. Thomas Telford Publishing, http://dx.doi.org/10.1680/doms.25844.

Storms, J.E., Weltje, G., van Dijke, J., Geel, C., Kroonenberg, S., 2002. Process-response modeling of wave-Dominated Coastal systems: Simulating evolution and stratigraphy on geological timescales. J. Sediment. Res. 72 (2), 226–239. http://dx.doi.org/10.1306/052501720226, http://arxiv.org/abs/https://pubs.geoscienceworld.org/sepm/jsedres/article-pdf/72/2/226/2814611/226.pdf.

U.S. Army Corps of Engineers, 2002. Coastal Engineering Manual, Engineer Manual 1110-2-1100. US Army Corps of Engineers, Washington, D.C..

Vos, K., Harley, M.D., Splinter, K.D., Walker, A., Turner, I.L., 2020. Beach slopes from satellite-derived shorelines. Geophys. Res. Lett. 47 (14), e2020GL088365.

de Vriend, H., Bakker, W., Bilse, D., 1994. A morphological behaviour model for the outer delta of mixed-energy tidal inlets. Coast. Eng. 23, 305–327. http://dx.doi.org/10.1016/0378-3839(94)90008-6.

Walstra, D.-J., Roelvink, D.J., Groeneweg, J., Calculation of wave-driven currents in a 3d mean flow model, vol. 276 (2000). https://doi.org/10.1061/40549(276)81.

Wang, H., Miao, G., Lin, L.-H., 1993. A time—Dependent nearshore morphological response model. pp. 2513–2527. http://dx.doi.org/10.1061/9780872629332.192.

Watanabe, A., Maruyama, K., Shimizu, T., Sakakiyama, T., 1986. Numerical prediction model of three-dimensional beach deformation around a structure. Coast. Eng. J. 29, 179–194. http://dx.doi.org/10.1080/05785634.1986.11924437.

Williams, J., Esteves, L., Rochford, L., 2015. Modelling storm responses on a high-energy coastline with XBeach. Model. Earth Syst. Environ. 1, http://dx.doi.org/10.1007/s40808-015-0003-8.

Yamaguchi, M., Nishioka, Y., 1985. Numerical simulation on the change of bottom topography by the presence of coastal structures. pp. 1732–1748. http://dx.doi.org/10.1061/9780872624382.118.

Zimmermann, N., Trouw, K., Wang, L., Mathys, M., Delgado, R., Verwaest, T., 2012. Longshore transport and sedimentation in a navigation channel at blankenberge (Belgium). Coast. Eng. Proc. 1, http://dx.doi.org/10.9753/icce.v33.sediment.111.

Zyserman, J., Johnson, H., 2002. Modelling morphological processes in the vicinity of shore-parallel breakwaters. Coast. Eng. 45, 261–284. http://dx.doi.org/10.1016/S0378-3839(02)00037-6.